Journal Name

COMMUNICATION

Imaging plasma membrane phase behaviour in live cells using a thiophene-based molecular rotor

Received 00th January 20xx,
Accepted 00th January 20xx

DOI: 10.1039/x0xx00000x

www.rsc.org/

Michael R. Dent,[a] Ismael López-Duarte,[a, b] Callum J. Dickson,[c]* Phoom Chairatana,[b] Harry L. Anderson,[b] Ian R. Gould,[a] Douglas Wylie,[a] Aurimas Vyšniauskas,[a] Nicholas J. Brooks[a]* and Marina K. Kuimova[a]*

Molecular rotors have emerged as versatile probes of microscopic viscosity in lipid bilayers, although it has proved difficult to find probes that stain both phases equally in phase-separated bilayers. Here, we investigate the use of a membrane-targeting viscosity-sensitive fluorophore based on a thiophene moiety with equal affinity for ordered and disordered lipid domains to probe ordering and viscosity within artificial lipid bilayers and live cell plasma membranes.

As the physical boundary separating the interior of a cell from the external environment, the plasma membrane plays a vital role in the function of a cell, by controlling access to and from its interior. The plasma membrane is a complex mixture of lipids and membrane proteins. The lipids were once thought to play a purely passive role,[1] but it is now believed that they are integral to the normal functioning of the cell, affecting processes such as cell division, signal transduction and protein aggregation.

Despite the apparent importance of the plasma membrane lipids, their supramolecular structures and lateral organisation are not yet well understood. Plasma membrane lipids are widely believed to transiently phase separate into coexisting, sub-micron ordered (L_o) and disordered (L_d) liquid domains, the so-called "lipid raft hypothesis",[2] where cholesterol rich L_o domains form platforms that function in membrane signalling and trafficking.[3] Despite growing evidence for phase separation within the plasma membrane and the demonstration of L_o-L_d phase separation in artificial membranes made up of plasma membrane extracts,[3–6] it is very difficult to directly observe this phase separation *in vivo*, mainly owing to the fact that the L_o domains are believed to have dimensions that are smaller than the diffraction limit of visible light,[6] with lifetimes on the microsecond timescale.[5,7,8]

Fluorescence techniques provide a non-invasive way to investigate plasma membrane structure and organisation, and have found widespread application in recent years.[9] Various fluorescence studies have found evidence for sub-resolution ordered regions within cell membranes,[6] with a recent study suggesting that up to 76% of the plasma membrane lipids may be in an L_o phase at any one time.[10]

An emerging fluorescence-based technique for investigating order and structure within biological systems is the use of molecular rotors, which are environmentally responsive fluorophores that show increased quantum yield and fluorescence lifetime within more viscous, ordered environments.[11] In general, after optical excitation, a molecular rotor can undergo either radiative or nonradiative decay. The rate of nonradiative decay, which typically occurs via an intramolecular rotation pathway, is directly affected by the friction imparted on the rotor by the surrounding environment. The competition between radiative and nonradiative decay leads to the environmentally sensitive fluorescence properties of the rotor.[11]

Viscosity can be related to fluorescence quantum yield using the Förster-Hoffmann equation,[12] however, monitoring fluorescence intensity alone does not allow measurement of viscosity in a concentration-independent manner. On the other hand, the fluorescence lifetime of a molecular rotor is unaffected by concentration, and can be related to the viscosity of its surrounding environment using a variant on the Förster-Hoffmann equation, shown in equation (1):[13, 14]

$$\log \tau_f = \log\left(\frac{z}{k_r}\right) + \alpha \log \eta \qquad (1)$$

where τ_f represents the fluorescence lifetime, η the viscosity,

[a] *Department of Chemistry, Imperial College London, Exhibition Road, London, SW7 2AZ, UK. E-mail:* m.kuimova@imperial.ac.uk; n.brooks@imperial.ac.uk
[b] *Department of Chemistry, Oxford University, Chemistry Research Laboratory, Oxford, UK OX1 3TA*
[c] *Computer-Aided Drug Discovery, Global Discovery Chemistry, Novartis Institutes for BioMedical Research, 100 Technology Square, Cambridge, MA 02139, USA.E-mail: callum.dickson@novartis.com*

Electronic Supplementary Information (ESI) available: materials and methods; additional spectroscopic and computational data. See DOI: 10.1039/x0xx00000x

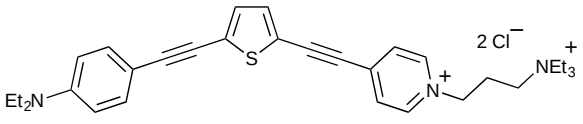

Fig. 1 Molecular structure of thiophene-based molecular rotor **1**

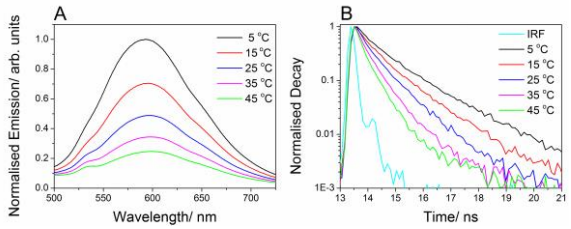

Fig. 2 Overlaid emission spectra (A) and normalised fluorescence decays (B) of **1** in DOPC LUVs at a range of temperatures.

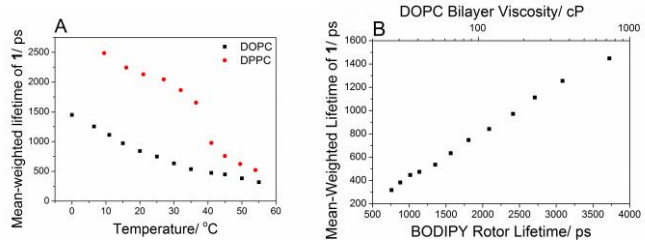

Fig. 3 (A) Mean weighted lifetime of **1** in DOPC and DPPC LUVs with temperature; (B) "viscosity calibration" of **1** by comparing mean weighted lifetime of **1** in DOPC LUVs with lifetimes of a well characterised BODIPY-based molecular rotor.[24]

k_r the radiative decay constant, and α and z are constants specific to that particular molecule.

Therefore, fluorescence lifetime imaging microscopy (FLIM), in conjunction with molecular rotors, can be used to generate a map of fluorescent lifetimes over a heterogeneous sample, in a concentration independent manner.[14] This technique has previously been used to image viscosity across a diverse array of heterogeneous systems, including atmospheric aerosols,[15] lipid monolayers and bilayers,[16] blood plasma,[17] and live mammalian and bacterial cells.[13, 14, 18–22]

In order to investigate viscosity and ordering within lipid bilayers, a range of BODIPY-based molecular rotors have been developed for FLIM studies. While these rotors enabled imaging of L_o-L_d phase separation[23] and determination of viscosity and diffusion coefficients within model bilayer systems,[24] the staining of the L_o phase was poor. Similarly to the majority of membrane probes and all molecular rotors reported to date,[9] BODIPY dyes are widely reported to partition into L_d phases, potentially limiting their utility as probes of membrane phase separation.[25]

Generally, attempts to quantitatively assess viscosity and ordering within the plasma membranes of eukaryotic cells have met with limited success,[26] with dyes either rapidly internalising into the cell interior,[13,27,28] or displaying poor partitioning between membrane phases.[23,24] A molecular rotor that targets the plasma membrane and partitions equally between different liquid phases could help to shed further light on the lateral organisation of lipids within the plasma membrane and the lipid raft hypothesis.

Recently, a range of D-π-A push-pull dyes were designed and synthesised with a thiophene group acting as the π-conjugated linking unit.[29] These dyes were found to preferentially stain the plasma membranes of live cells for prolonged periods of time, with low dark toxicity (in particular, **1**, Fig. 1), which enabled efficient two photon fluorescence and second harmonic generation (SHG) imaging of cellular membranes.[29] Here, we test the hypothesis that, based on its push-pull structure, the thiophene based dye **1** may be capable of acting as a viscosity-sensitive molecular rotor.

The viscosity-sensitivity of **1** was first tested in large unilamellar vesicles (LUVs) made from of 1,2-dioleoyl-*sn*-glycero-3-phosphocholine (DOPC), at temperatures in the range 5-60 °C, Fig. 2. DOPC is an unsaturated lipid that forms liquid-disordered phase (L_d) bilayers at room temperature, and does not undergo any phase transitions in the temperature range studied.[30] Using BODIPY-based molecular rotors, we have previously[24] established that in this temperature range the viscosity of the tail region of the DOPC bilayer changes between 30 and 675 cP, Fig. 3. As can be clearly seen from Fig. 2, the fluorescence intensity of **1** increases significantly with increasing viscosity, confirming that **1** behaves as a molecular rotor. Similarly, the fluorescence decay times of **1** lengthen significantly at lower temperatures, Fig. 2, suggesting that **1** is a suitable probe for lifetime imaging of viscosity.

We then tested LUVs made from 1,2-dipalmitoyl-sn-glycero-3-phosphocholine (DPPC), a saturated lipid which forms gel phase (S_o) bilayers at room temperature with a gel-to-liquid phase transition temperature at 41 °C. Again, the emission intensity of **1** decreased with increasing temperature (Fig. S2, ESI), showing a clear transition at around 40 °C, corresponding with the gel-to-liquid phase transition.

Unlike the BODIPY-based molecular rotors,[24] **1** displays a biexponential fluorescence decay profile in all lipid systems studied (Fig. 2 and Fig. S3, ESI). The mean-weighted fluorescence lifetime was calculated from both lifetime components (τ_i) and their amplitudes (α_1) using the equation:

$$\tau_{mean-weighted} = \frac{\tau_1^2\alpha_1+\tau_2^2\alpha_2}{\tau_1\alpha_1+\tau_2\alpha_2} \quad (2)$$

A plot of mean lifetime against temperature can be seen in Fig. 3. While the trend is smooth for **1** in DOPC, the sharp change in gradient for DPPC at ca. 40 °C reflects the gel-to-fluid transition temperature.

We then went on to compare the mean-weighted lifetime of **1**, recorded in DOPC at variable temperature, with the fluorescence lifetimes of a well-characterised BODIPY based rotor under identical conditions[24,26] (Fig. 3). This allowed the viscosity sensitivity of **1** to be calibrated within a lipid bilayer, and is based upon the fact that both dyes occupy a very similar position within the bilayer (see Fig. S14, ESI, and below for further discussion of molecular dynamics simulations). This approach was used as **1** is insoluble in highly nonpolar viscous solvents such as castor oil, which can provide a required range of viscosities at variable temperature for calibration purposes. On the other hand, polar solvent mixtures such as methanol/glycerol are not suitable for applications of **1** to lipid bilayer viscosity measurements, due to the polarity sensitivity of **1**.[29]

On a double logarithmic scale, there is linear correlation between the fluorescence lifetime of **1** and the membrane viscosity (derived from the fluorescence lifetime of a BODIPY rotor[24]) in agreement with equation (1), confirming that **1** does

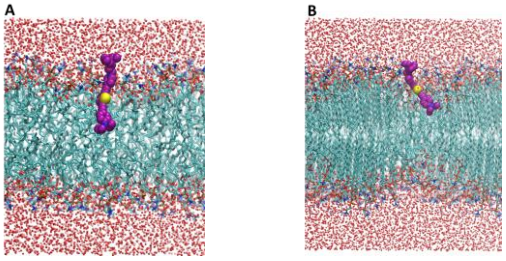

Fig. 4 Molecular dynamics simulations showing the orientations of **1** in (A) DOPC and (B) DPPC bilayers at 23 °C.

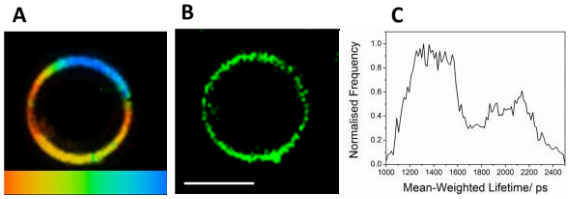

Fig. 5 (A) Fluorescence lifetime image (the colour hue mean-weighted lifetime range is between 1250-2150 ps) and (B) confocal image (scale bar = 20 μm) of a phase-separating GUV stained with **1**; (C) a histogram showing the fluorescence lifetime distribution across 10 phase-separating GUVs.

indeed act as a molecular rotor, and its mean lifetime can be correlated to the bilayer viscosity.

In order to probe the orientation and position of **1** within the bilayer, the molecular dynamics (MD) software AMBER[31,32] was used to simulate the behaviour of **1** within a lipid bilayer, with the final configuration in pure DOPC and DPPC bilayers shown in Fig. 4. We have also investigated the changes in orientation of **1** in both bilayers upon addition of cholesterol, up to 50 mol%, and at a range of temperatures between 5 and 60 °C, see ESI Section (3) for more details. By comparing the orientation of **1** in the DOPC bilayer with that of a well-studied BODIPY rotor (Fig. S14, ESI, structure shown in Fig. S15, ESI),[24] we found that the rotating units of the two dyes occupy essentially the same position within bilayer. Therefore, using the viscosity derived from the lifetime of the BODIPY rotor for the calibration of responses of **1** to viscosity (Fig. 3) is, indeed, valid.

To investigate the partitioning of **1** into L_o and L_d phases, we prepared phase-separating ternary giant unilamellar vesicles (GUVs) consisting of DOPC/DPPC/cholesterol in a 1:1:1 molar ratio using electroformation.[33] Confocal images show equal dye partitioning in both phases (Fig. S16, ESI), while lifetime images show clear differentiation between L_o and L_d phases from the lifetime of **1** (Fig. 5 and Fig. S17, ESI). The L_o and L_d phases display mean lifetimes of 2090 ps and 1380 ps, respectively, across 10 GUV images, suggesting that L_o phases are significantly more viscous, in agreement with previous studies with molecular rotors.[23,24] Importantly, the pixel-by-pixel fluorescence intensity from the L_o phases is comparable to that from the L_d phases, and suggests that **1** partitions roughly equally between the two phases, in contrast to other molecular rotors reported to date.

1 was then introduced into the membranes of six cell lines: BE, HCT 116, NIH 3T3, neuroblastoma, HeLa and SK-OV-3, in order to investigate its fluorescent properties within cells. In agreement with the previous work,[29] **1** localises primarily within the plasma membrane of each of the cell lines, allowing lifetime imaging of the plasma membranes (Fig. 6). Summed normalised histograms showing the mean-weighted lifetime distribution of 10 images for each cell line are shown in Fig. 6E. The mean lifetimes for BE, HCT 116, NIH 3T3, neuroblastoma, HeLa and SK-OV-3 cell membranes were and 1725, 1710, 1786 1758, 1671 and 1378 ps, respectively. Even though the data from SK-OV-3 cells is an outlier (see Fig. S18, ESI), these mean lifetime values of **1** in all cells are between values expected for L_o and L_d phases from studies in model membranes, and may imply a mixture of coexisting L_o and L_d phases within each pixel of the lifetime image. Individual lifetime images of plasma membranes for each of the four cell lines certainly appear to be homogeneous (Fig. 6), suggesting that any L_o-L_d phase separation, if present, is below the optical resolution of the microscope, or below the temporal resolution of the FLIM technique, which used a collection time of 300 seconds for each image.

Given possible parameter uncertainties in fitting the biexponential decays of **1**, and in order to further investigate the possibility of the existence of coexisting lipid phases, we used phasor analysis[34] to compare fluorescence decays of **1** within model L_o phases (DPPC/cholesterol LUVs) and model L_d phases (DOPC/cholesterol LUVs), Fig. S5, ESI and the plasma membranes of the live cell lines (Fig. 7). Phasor analysis[34] is a model-free approach that uses Fourier transforms of time-resolved fluorescence decays to produce a decay representation in a phasor space, on the universal circle. This approach is free from uncertainties introduced by choosing a (multi)exponential decay model, and does not require multi-parameter fitting. The decays recorded for **1** in live cell plasma membranes fell on the straight line between the pure L_o

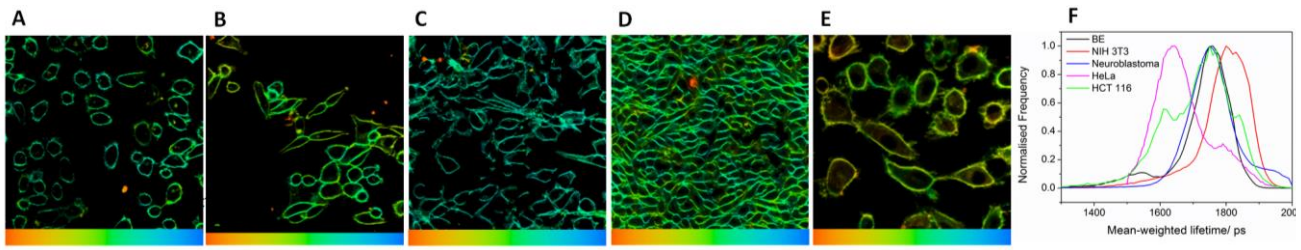

Fig. 6 Sample fluorescence lifetime images of BE (A), HCT 116 (B), NIH 3T3 (C), neuroblastoma (D) and HeLa (E) live cells, the colour hue mean-weighted lifetime range is between 1250-2150 ps; (F) histogram of a mean weighted lifetime showing distribution for the four cell lines, averaged over 10 images.

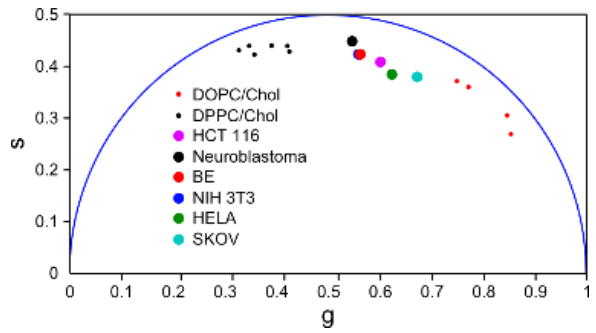

Fig. 7 Phasor transforms of fluorescence decays of **1** in model membranes and the membranes of living cells. The model membranes were LUVs composed of DOPC (red points – model L_d phases) and DPPC (black points – model L_o phases) lipids with varying amounts of cholesterol. The phasor points of **1** in living cells (large circles) were obtained by phasor transforming a set of 10 FLIM images of **1** in each cell line.

phases, formed from DPPC/Cholesterol mixtures, and the pure L_d phases, formed from DOPC/Cholesterol mixtures. This result strongly suggests a coexisting mixture of the two phases in plasma membranes of live cells, consistent with recent studies.[7,10]

In conclusion, we have investigated a thiophene-based molecular rotor **1**, which selectively stains the plasma membrane of live cells. By comparing the fluorescence lifetime of this rotor in cell membranes with model bilayers we have inferred the existence of coexisting ordered and disordered regions within the cell plasma membranes, below either the spatial or temporal resolution of the microscope.

MKK thanks to the EPSRC for a Career Acceleration Fellowship (EP/I003983/1). This work was partially supported by the European Commission in the form of a Marie Curie individual fellowship to ILD under the contract PIEF-GA-2009-255164.

References

1. S. J. Singer and G. L. Nicolson, *Science*, 1972, **175**, 720–731.
2. K. Simons and E. Ikonen, *Nature*, 1997, **387**, 569–572.
3. D. Lingwood and K. Simons, *Science*, 2010, **327**, 46–50.
4. S. Sonnino and A. Prinetti, *Curr. Med. Chem.*, 2013, **20**, 4–21.
5. J. F. Hancock, *Nat. Rev. Mol. Cell Biol.*, 2006, **7**, 456–462.
6. D. M. Owen, A. Magenau, D. Williamson and K. Gaus, *Bioessays*, 2012, **34**, 739–747.
7. C. Eggeling, C. Ringemann, R. Medda, G. Schwarzmann, K. Sandhoff, S. Polyakova, V. N. Belov, B. Hein, C. von Middendorff, A. Schönle and S. W. Hell, *Nature*, 2009, **457**, 1159–1162.
8. S. J. Sahl, M. Leutenegger, M. Hilbert, S. W. Hell and C. Eggeling, *Proc. Natl. Acad. Sci. U. S. A.*, 2010, **107**, 6829–6834.
9. A. S. Klymchenko and R. Kreder, *Chem. Biol.*, 2014, **21**, 97–113.
10. D. M. Owen, D. J. Williamson, A. Magenau and K. Gaus, *Nat. Commun.*, 2012, **3**, 1256.
11. M. K. Kuimova, *Phys. Chem. Chem. Phys.*, 2012, **14**, 12671–12686.
12. T. Förster and G. Hoffmann, *Z. Phys. Chem*, 1971, **75**, 63–76.
13. M. K. Kuimova, G. Yahioglu, J. A. Levitt and K. Suhling, *J. Am. Chem. Soc.*, 2008, **130**, 6672–6673.
14. M. K. Kuimova, *Phys. Chem. Chem. Phys*., 2012, **14**, 12671-12686.
15. N. A. Hosny, C. Fitzgerald, C. Tong, M. Kalberer, M. K. Kuimova and F. D. Pope, *Faraday Discuss.*, 2013, **165**, 343–356.
16. N. A. Hosny, G. Mohamedi, P. Rademeyer, J. Owen, Y. Wu, M. X. Tang, R. J. Eckersley, E. Stride and M. K. Kuimova, *Proc. Natl. Acad. Sci. U. S. A.*, 2013, **110**, 9225–9230.
17. W. J. Akers, J. M. Cupps and M. A. Haidekker, *Biorheology*, 2005, **42**, 335–344.
18. E. Gatzogiannis, Z. Chen, L. Wei, R. Wombacher, Y. T. Kao, G. Yefremov, V. W. Cornish and W. Min, *Chem. Commun.*, 2012, **48**, 8694–8696.
19. G. Ferri, L. Nucara, T. Biver, A. Battisti, G. Signore and R. Bizzarri, *Biophys. Chem.*, 2016, **208**, 17–25.
20. S. Raut, J. Kimball, R. Fudala, H. Doan, B. Maliwal, N. Sabnis, A. Lacko, I. Gryczynski, S. V Dzyuba and Z. Gryczynski, *Phys. Chem. Chem. Phys.*, 2014, **16**, 27037–27042.
21. X. Peng, Z. Yang, J. Wang, J. Fan, Y. He, F. Song, B. Wang, S. Sun, J. Qu, J. Qi and M. Yan, *J. Am. Chem. Soc.*, 2011, **133**, 6626–6635.
22. M. K. Kuimova, S. W. Botchway, A. W. Parker, M. Balaz, H. A. Collins, H. L. Anderson, K. Suhling and P. R. Ogilby, *Nat. Chem.*, 2009, **1**, 69–73.
23. Y. Wu, M. Štefl, A. Olzyńska, M. Hof, G. Yahioglu, P. Yip, D. R. Casey, O. Ces, J. Humpolíčková and M. K. Kuimova, *Phys. Chem. Chem. Phys.*, 2013, **15**, 14986–14993.
24. M. R. Dent, I. López Duarte, C. J. Dickson, N. D. Geoghegan, J. M. Cooper, I. R. Gould, R. Krams, J. A. Bull, N. J. Brooks and M. K. Kuimova, *Phys. Chem. Chem. Phys.*, 2015, **17**, 18393–18402.
25. V. Kilin, O. Glushonkov, L. Herdly, A. Klymchenko, L. Richert and Y. Mely, *Biophys. J.*, 2015, **108**, 2521–2531.
26. I. López-Duarte, T. T. Vu, M. A. Izquierdo, J. A. Bull and M. K. Kuimova, *Chem. Commun.*, 2014, **50**, 5282–5284.
27. M. Dakanali, T. H. Do, A. Horn, A. Chongchivivat, T. Jarusreni, D. Lichlyter, G. Guizzunti, M. A. Haidekker and E. A. Theodorakis, *Bioorg. Med. Chem.*, 2012, **20**, 4443–4450.
28. J. A. Levitt, M. K. Kuimova, G. Yahioglu, P. H. Chung, K. Suhling and D. Philips, *J. Phys. Chem. C*, 2009, **113**, 11634–11642.
29. I. López-Duarte, P. Chairatana, Y. Wu, J. Pérez-Moreno, P. M. Bennett, J. E. Reeve, I. Boczarow, W. Kaluza, N. A. Hosny, S. D. Stranks, R. J. Nicholas, K. Clays, M. K. Kuimova and H. L. Anderson, *Org. Biomol. Chem.*, 2015, **13**, 3792–3802.
30. S. Kaneshina, H. Ichimori, T. Hata and H. Matsuki, *Biochim. Biophys. Acta*, 1998, **1374**, 1–8.
31. C. J. Dickson, B. D. Madej, Å. A. Skjevik, R. M. Betz, K. Teigen, I. R. Gould and R. C. Walker, *J. Chem. Theory Comput.*, 2014, **10**, 865–879.
32. D. A. Case, V. Babin, J. T. Berryman, R. M. Betz, Q. Cai, D. S. Cerutti, T. E. Cheatham III, T. A. Darden, R. E. Duke, H. Gohlke, A. W. Goetz, S. Gusarov, N. Homeyer, P. Janowski, J. Kaus, I. Kolossváry, A. Kovalenko, T. S. Lee, S. Le Grand, T. Luchko, R. Luo, B. Madej, K. M. Merz, F. Paesani, D. R. Roe, A. Roitberg, C. Sagui, R. Salomon-Ferrer, G. Seabra, G. L. Simmerling, W. Smith, J. Swails, R. C. Walker, J. Wang, R. M. Wolf, X. Wu and P. A. Kollman, *AMBER 14*, 2014, University of California, San Francisco.
33. L. A. Bagatolli, T. Parasassi and E. Gratton, *Chem. Phys. Lipids*, 2000, **105**, 135–147.
34. M. A. Digman, V. R. Caiolfa, M. Zamai and E. Gratton, *Biophys. J.*, 2008, **94**, L14–L16.

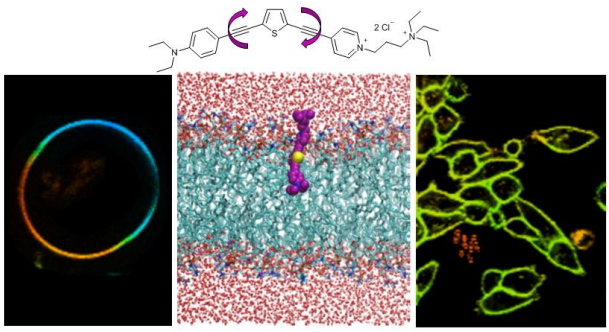

A thiophene-based molecular rotor was used to probe ordering and viscosity within artificial lipid bilayers and live cell plasma membranes